RESEARCH PAPER

# *In Vitro* Antimicrobial, Antioxidant and *In Vivo* Wound Healing Activity on Wistar Albino Rats by Plant-Mediated Synthesis of CuO Nanoparticles from the Fruit Extract of *Diplocyclos palmatus (L) C. Jeffrey*

***Parethe Gurusamy Thangam[1], Rajesh Pattulingam [1*], Kavica Sathasivam[1], Balaji Murugesan[1], Velmani Vellaiyan[1]***

*[1]PG& Research Department of Chemistry, Government Arts College, Coimbatore-18, Tamil Nadu, India*

## ABSTRACT

This study investigates the in vitro antimicrobial, antioxidant, and in vivo wound healing activities of copper oxide (CuO) nanoparticles synthesized from the Diplocyclos palmatus (L) C. Jeffrey fruit extract. A nanoemulsion containing CuO nanoparticles was prepared and tested for its efficacy in healing deep skin wounds in a rat model. Wound healing is a significant area of public health concern. Plant-mediated synthesis of metal oxide nanoparticles has minimized side effects while exhibiting superior biological activities compared to traditional synthetic methods. In this research, the fruit extracts of D. palmatus were employed to synthesize CuO nanoparticles, which were then evaluated for their in vitro antibacterial activities against both Gram-positive and Gram-negative bacteria, antifungal properties, and antioxidant activity. The prepared nanoemulsion ointment was tested in a rat wound healing model. The synthesized nanoparticles were characterized using UV-vis spectroscopy, FT-IR, XRD, SEM & EDX, DLS, and minimum inhibitory concentration (MIC) assays. The CuO nanoparticles demonstrated significant antibacterial activity against Staphylococcus aureus (11 mm zone of inhibition) and effective antifungal activity against Candida albicans. The antioxidant activity, measured using the DPPH radical scavenging assay, reached 80.39% at a 100 µg/mL concentration. MIC values for Streptococcus aureus and Escherichia coli were determined to be 20 µg/mL and 40 µg/mLmL, respectively. CuO-NP-based ointments facilitated complete wound healing (100%) in 28 days, compared to the control group (Group I). Histopathological analysis further confirmed the wound healing efficacy of the CuO nanoparticles.

***Keywords:*** *Copper oxide nanoparticles, Diplocyclos palmatus fruit, Ointment, Public health, Rats, Wound healing*

**How to cite this article**

*Gurusamy Thangam P, Pattulingam R, Sathasivam K, Murugesan B, Vellaiyan V. In Vitro Antimicrobial, Antioxidant and In Vivo Wound Healing Activity on Wistar Albino Rats by Plant-Mediated Synthesis of CuO Nanoparticles from the Fruit Extract of Diplocyclos palmatus (L) C. Jeffrey. Nanomed J. 2025; 12: 1-. DOI: 10.22038/nmj.2025.79388.1956*

**Abbreviation**

CuO-Copper oxide, CuSO4.5H2O- Copper Sulphate pentahydrate, D. palmatus - Diplocyclos palmatus (L) C. Jeffrey, MIC-Minimum inhibitory concentration, NPs- Nanoparticles, FTIR- Fourier Transform Infra-Red Spectroscopy, SEM-Scanning Electron Microscopy, EDX- Energy Dispersive Spectrometry, DLS- Dynamic Light Scattering.

**Graphical Abstract**

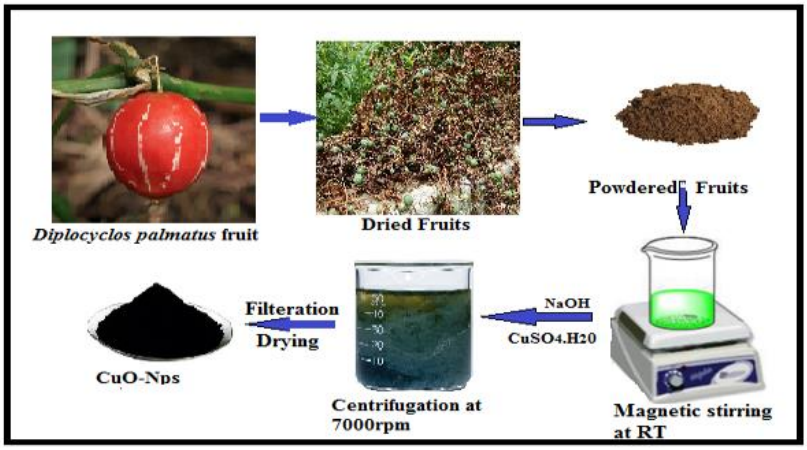


*Corresponding author(s) Email: gacchemistryrajesh@gmail.com

Note. This manuscript was submitted on April 17, 2024;approved on June 19, 2024

## INTRODUCTION

Since the incidence of infectious diseases is dramatically increasing, effective germ control is crucial for public health protection. Infections are widespread health issues in developing countries, where they strain health systems, reduce life expectancy, and impede economic progress [1]. According to a 2019 report, an estimated 13.7 million deaths worldwide were attributed to infectious diseases [2]. To curb the spread of these diseases, preventive measures such as vaccinations, proper hygiene, and antibiotic therapy have been developed in recent years [3–5]. In India, a survey found that over 33% of the population suffers from infectious diseases. Wound healing is a natural process; however, it is slow and increases the risk of microbial infection. Therefore, accelerating the healing process is essential. Natural remedies for cuts, burns, and wounds have gained popularity in recent years. Compared to pharmaceutical treatments, medicinal herbs have been shown to promote more effective wound healing [6]. Recently, nanomaterials have emerged as a promising area in wound healing therapy. Among them, bioactive nanoparticles are favored for their cost-effectiveness, biocompatibility, low toxicity, and favorable surface-to-volume ratio [7]. More sustainable and environmentally friendly methods are now being encouraged. Although chemical processes can produce well-defined nanoparticles, they are often expensive and generate harmful waste [8]. In contrast, plant-mediated synthesis of nanoparticles yields environmentally safe materials with minimal hazards [9, 10]. Researchers have demonstrated that greener synthetic methods produce superior products to traditional chemical processes [11]. Nanoparticles are known for their long shelf life, making them suitable for both in vivo and in vitro medical applications. Copper-based nanoparticles have shown considerable promise in medicinal uses due to their antimicrobial properties and are widely used in advanced antimicrobial formulations. Specifically, copper oxide nanoparticles (CuO-NPs) have gained significant attention in various studies due to their remarkable potential in several medical applications [12–14]. CuO-NPs synthesized from green sources, with particle sizes less than 100 nm, have demonstrated excellent antibacterial activity [15]. These nanoparticles are extensively utilized for their antibacterial, antifungal, antioxidant, and wound healing properties [16].

Traditionally, medicinal plants have served as an essential source of organic bioactive compounds. *Diplocyclos palmatus* (L) C. Jeffrey, a member of the Cucurbitaceae family, is a notable medicinal plant known for its rich cucurbitacins and tetracyclic triterpenes [17]. Cucurbitacins, unsaturated terpenes, contain many keto-, hydroxyl-, and acetoxy groups [18]. This plant has a long history of use in traditional medicine, where it is recognized for its laxative, expectorant, anticonvulsant, anti-venom, antibacterial, and analgesic properties [19]. The phytochemicals found in its fruits are utilized in the synthesis of nanoparticles, as detailed in Table 1 [20, 21].

## MATERIALS AND METHODS

### *Preparation of fruit extracts*

The fruits of *D. palmatus* were harvested, washed with tap water followed by distilled water, and then dried for forty days to remove contaminants. After drying, the fruits were ground into a fine powder using a blender. To prepare the extract, 300 mL of distilled water was added to approximately 30 g of the fruit powder, and the mixture was stirred for three hours using a magnetic stirrer. The solution was then filtered using Whatman filter paper No. 1. The resulting fruit extract was stored to further synthesize metal oxide nanoparticles.

Table 1. Preliminary Phytochemical study of D.palmatus fruits

| S.No | Phytochemical constituents | Aqueous extract |
|---|---|---|
| 1 | Alkaloids | + |
| 2 | Flavonoids | + |
| 3 | Sugars | - |
| 4 | Saponins | + |
| 5 | Steroids | + |
| 6 | Proteins | + |
| 7 | Resins | - |
| 8 | Starch | - |

### *Chemical synthesis of CuO nanoparticles*

Copper oxide nanoparticles were synthesized at room temperature using a 1 M aqueous solution of $CuSO_4 \cdot 5H_2O$, with NaOH as the stabilizing agent and $NaBH_4$ as the reducing agent. Black-colored nanoparticles were formed and then centrifuged, dried, and collected.

### *Green synthesis of CuO nanoparticles*

Plant-mediated synthesis was employed to produce copper oxide nanoparticles (CuO-NPs). The fruit extracts of *D. palmatus* served effectively as capping agents during synthesis. A 1 M aqueous solution of 35 mL $CuSO_4 \cdot 5H_2O$ was added to 30 mL of fruit extract and stirred for 10 minutes. NaOH was then added to the mixture until the pH reached the desired level, and a color change in the solution

was observed. The mixture was centrifuged at 7,000 rpm, yielding a pellet containing CuO-NPs. The pellet was thoroughly washed with distilled water to remove any remaining contaminants and dried in a hot air oven at 70 °C. The characteristics, as well as the antibacterial, antioxidant, and wound-healing properties of the dried CuO-NPs, were subsequently investigated.

***Characterization***

The absorption band of CuO-NPs was studied using a UV-visible spectrophotometer. The surface functionalization of CuO-NPs was examined using FT-IR (Shimadzu IR Affinity Model 1S, double beam spectrometer). XRD (Empyrean, Malvern Panalytical) analyzed the crystalline nature and phase identification with CuKα (λ = 1.54 Å) radiation. The prepared nanoparticles' surface morphology and particle size were characterized using scanning electron microscopy (SEM) (Carl Zeiss, USA, Model Sigma with Gemini column). EDX analysis was performed to determine the elemental composition of CuO-NPs.

***Antimicrobial Analysis***

***Anti-bacterial activity by Disc diffusion assay***

The antibacterial activity of the synthesized CuO-NPs was evaluated against the bacterial strains *Pseudomonas aeruginosa*, *Staphylococcus aureus*, *Staphylococcus epidermidis*, and *Klebsiella pneumoniae*, which were obtained from the Microbial Type Culture and Collection (MTCC) in Chandigarh. The disc diffusion method was employed to assess the antibacterial efficacy of CuO-NPs. A 10 mL aliquot of Mueller-Hinton agar solution was poured into 60 mm sterile Petri dishes, and the test organisms were then inoculated. Different concentrations of CuO-NPs (60, 80, and 100 µg/mL) were loaded onto sterile filter paper discs and placed on the surface of the Mueller-Hinton agar plates. Amoxicillin was used as a positive control. After incubating the plates at 37°C for 24 hours, the zone of inhibition was measured in millimeters [22].

***Antifungal activity by the Disc diffusion assay***

The antifungal activity of the synthesized CuO-NPs was evaluated using the test species *Aspergillus niger*, *Aspergillus flavus*, *Candida albicans*, and *Candida vulgaris*. The disc diffusion method was employed for this analysis. Test organisms were inoculated onto 60-mm Petri dishes containing Sabouraud's dextrose agar [23]. CuO-NPs at 60, 80, and 100 µg/mL concentrations were impregnated into sterile discs. The discs were then incubated at 37°C for 24 hours [24]. Fluconazole was used as the positive control. The zone of inhibition was measured in millimeters.

***Anti-oxidant analysis***

The antioxidant potential of CuO-NPs was evaluated using the DPPH free radical assay. A 500 µL aliquot of 0.05 M ethanolic DPPH solution was mixed with 1000 µL of CuO-NPs solution at varying concentrations (20-100 µg/mL) [25]. The freshly prepared DPPH solution was stored at 4°C in the dark. After adding 2.7 mL of 96% ethanol to the mixture and allowing it to stand for 5 minutes, the absorbance was measured at 540 nm. The radical scavenging activity of CuO-NPs was expressed as the percentage of inhibition [26].

Percent (%) inhibition of DPPH activity = [(A-B)/A] x 100 (1)

Where the absorbance values of the CuO-NPs and blank are denoted by A and B. A concentration versus percentage of inhibition curve was plotted.

***Minimum Inhibitory Concentration (MIC) analysis***

After inoculating with multiple specimens, about 2 mL of nutrient broth was added to each test tube. A 50 µL aliquot of different bacterial cultures, including *Escherichia coli* and *Streptococcus aureus*, was introduced into each test tube. Various concentrations of fruit extract (20, 40, 60, 80, and 100 µg/mL) were added to the test tubes. Common antibiotics, such as amoxicillin, were included as controls. The test tubes were incubated at 37°C for 24 hours to promote bacterial growth. After incubation, the test tubes were examined for turbidity, which indicates bacterial growth. Test tubes without turbidity, showing no visible growth, were considered to exhibit antimicrobial activity.(Table 2 and 3)

Table 2. Prototypes of Wound healing Ointment

| S.No | Ingredients | HLB value | Properties | Prototype (wt) |
|---|---|---|---|---|
| 1 | CuO-NPs | --- | Wound healing property | 0.002g |
| 2 | Stearic acid powder | 4.7 | Emulsifier | 1 g |
| 3 | Cera alba pellets | 1.7 | Thickener | 1 g |
| 4 | Lavender oil | 10 | Anti-inflammatory property | 1 ml |
| 5 | Water | | --- | q.s |
| 6 | Tea tree Oil | 2.3 | Anti-Oxidant property | 1 ml |

Table 3. Nanoemulsion Development

| |
|---|
| **Mixing:** |
| **1)** Preparation of aqueous and oil phase into a separate containers before mixing |
| **2)** Adding oil soluble preservative in oil phase and water soluble preservative in water phase |
| **3)** Adding aqueous phase to oil phase through wall of the container |
| **4)** Stirring the emulsion at constant temperature of (40°C to 45°C) for 30-40 min for proper emulsion |
| **Preparation of Aqueous phase:** |
| **1)** Aqueous phase ingredient is the synthesized CuO nanoparticles from the fruit extracts of *D.palmatus* is added to distilled water. |
| **Preparation of Oil phase:** |
| **1)** Adding stearic acid powder to the melting Cera alba wax followed by Tea tree oil. |
| **2)** Adding Lavender oil into the above prepared emulsion before mixing two phases |

***Wound healing activity***

***Animals***

Wistar albino rats, weighing between 200 and 250 g, were obtained from JSS College of Pharmacy in Ooty, India. The experimental protocols and procedures of the study were approved by the Institutional Animal Ethics Committee (JSSCP/OT/IAEC/53/2023-24) under the guidelines set by the Ministry of Environment and Forest, Government of India, and the Committee for Control and Supervision of Animal Experiments (CPCSEA). The rats were housed in standard polypropylene cages with a continuous water supply and regular nourishment. All procedures followed the ethical guidelines established by the Institutional Animal Ethics Committee. The animals were divided into two groups, each consisting of six rats. A 500 mm² wound was created by excising the full thickness of skin from the designated area, including the panniculus carnosus. Group I received treatment until the wound was completely healed, while Group II was the control. Body weights were recorded on days 0 through 28. Wound area was assessed on days 0, 1, 7, 14, 21, and 28 of the study. Statistical analysis was performed using GraphPad Prism 9 software, and the percentage of wound closure was calculated. Tukey's multiple comparison tests and two-way ANOVA were applied, with a p-value of less than 0.05 considered statistically significant.

Group I: Control animals (wound only)
Group II: Wound + Ointment

***Parameters observed***

***Body Weight***

The body weight of the animals was determined on days 0, 1, 7, 14, 21, and 28.

***Assessment of wound healing***

The physical characteristics of wound healing, including wound area and closure percentage, were evaluated by assessing the untreated wound. Wound area measurements were taken from Day 0 to Day 28. The percentage of wound closure was calculated using the following formula:

$$\%\ \text{Wound closure} = \frac{\text{Wound area on day 0} - \text{wound area on day N}}{\text{wound area on day 0}} \times 100 \quad (2)$$

Where N = wound area on the corresponding days

***Histopathological analysis***

After the study, wound tissues from each group were collected and preserved in 10% formalin. After the tissue sections were dehydrated in increasing concentrations of ethanol and lipid debris was removed by soaking in alcohol, the samples were embedded in paraffin wax. Thin coronal sections of wound tissue were cut using a microtome, measuring 5-10 µm in thickness. The sections were then stained with hematoxylin and eosin (H&E). The stained tissue sections were examined under a 40x Motic microscope, and images were captured to assess the changes in the wound tissue area caused by the different treatments [27].

**RESULTS**

***UV-visible spectroscopy***

CuO nanoparticles were synthesized using the metal reduction method, and the results were confirmed using a UV-visible spectrophotometer. Chemically synthesized CuO NPs exhibit a sharp surface plasmon resonance (SPR) spectral band at 370 nm. In contrast, the greenly synthesized CuO NPs display an SPR band at 274 nm, as shown in Figures 1a and 1b. SPR, which is highly sensitive to particle size, results from the oscillation of free electrons confined to the surface of the nanoparticles. Consequently, as the nanoparticle size decreases, the λ_max values decrease [28]. These findings are consistent with the crystallite sizes observed from the XRD peak broadening.

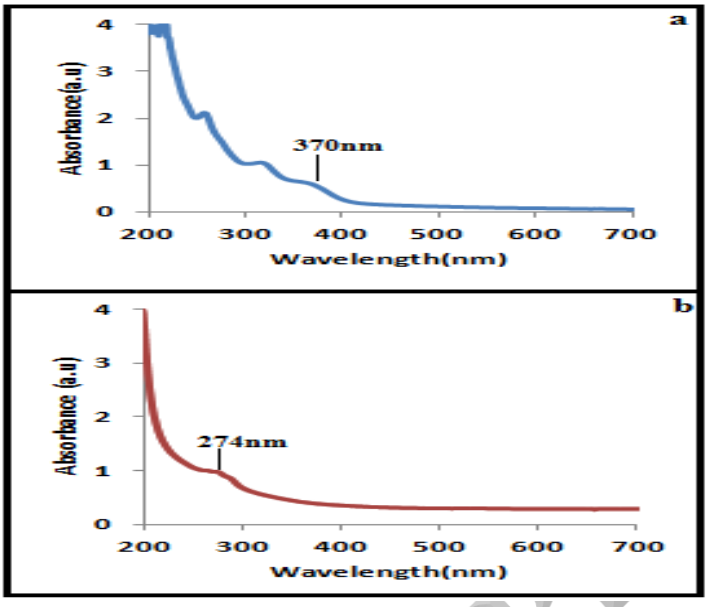


Fig. 1. UV-visible spectrum of chemical (a) and green synthesized (b) CuO-NPs

***Fourier-transform infrared spectroscopy***

FTIR measurements were performed to investigate the nature of the capping agent and the functional groups involved in the synthesis of CuO-NPs [28]. The FTIR spectra of CuO synthesized by conventional chemical methods showed characteristic peaks at 439 and 547 $cm^{-1}$, corresponding to CuO stretching (Figure 2a). The peak at 2911 $cm^{-1}$ is attributed to C-H stretching, which occurs on the CuO surface due to the alkane group. Additional 1697 and 1419 $cm^{-1}$ peaks are associated with OH bending and C=O stretching, respectively. Figure 2b shows the FTIR spectrum of green-synthesized CuO-NPs, with the peak corresponding to copper oxide observed between 437 and 540 $cm^{-1}$. The presence of lipids is indicated by the alkyl C-H stretching at 2924 $cm^{-1}$, while the peak at 1743 $cm^{-1}$ is due to C=O stretching in polysaccharides [29].

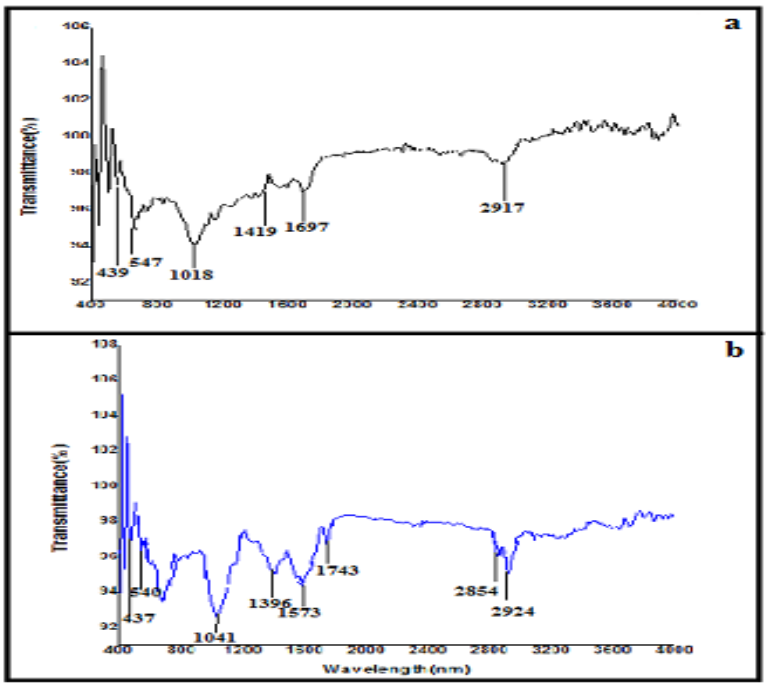


Fig. 2. FT-IR spectrum of chemical (a) and green synthesized (b) CuO-NPs

***XRD***

The crystal structure of the CuO nanoparticles was examined through XRD analysis. The lattice planes corresponding to (110), (111), (202), and (311), as shown in Figure 3, were observed at Bragg angles of 23.8°, 35.4°, 48.8°, and 66.1°, respectively. These peaks are consistent with the monoclinic phase of CuO nanoparticles (JCPDS No. 48-1548). The size of the nanoparticles was calculated using the Debye-Scherrer formula.

$$D = K\lambda / \beta\cos\theta \quad (3)$$

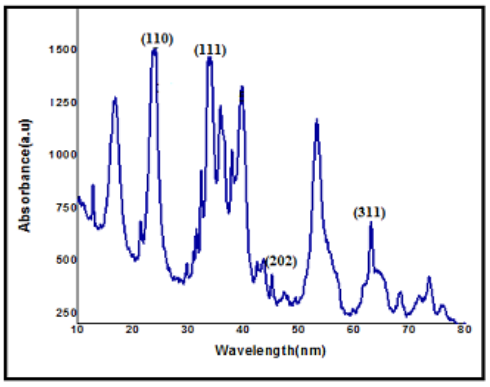


Fig. 3. XRD graph of prepared CuO nanoparticles

In this equation, D represents the particle size, K is a shape factor (approximately 0.9), λ is the X-ray wavelength (1.5418 Å with Cu K radiation), β is the full width at half maximum (FWHM) of the primary intensity peak, and θ is the Bragg's angle. The average particle size of the synthesized CuO-NPs was calculated to be 22 nm.

***SEM & EDX Analysis***

The surface morphology of CuO-NPs was examined using a scanning electron microscope (SEM). A rod-shaped stacked structure was observed in the CuO-NPs, as shown in Figures 4a and 4b [30]. The elemental composition of the CuO-NPs was determined using EDX analysis. Carbon and nitrogen were detected in the synthesized nanoparticles. As shown in Figure 4c, the weight percentages of copper and oxygen were 30% and 11%, respectively.

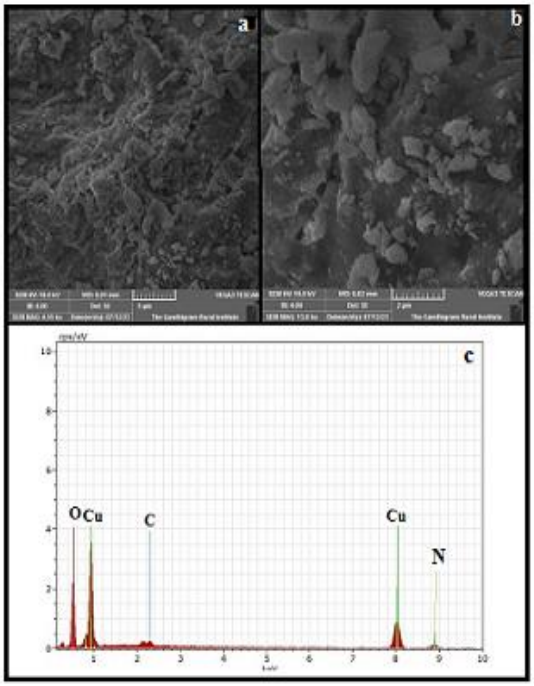


Fig. 4. Scanning Electron Microscopy image of CuO-NPs (a, b) and EDX spectrum (c)

***Particle size distribution***

The particle size distribution was analyzed using dynamic light scattering (DLS). As shown in Figure 5, the average particle size was approximately 68 nm [31].

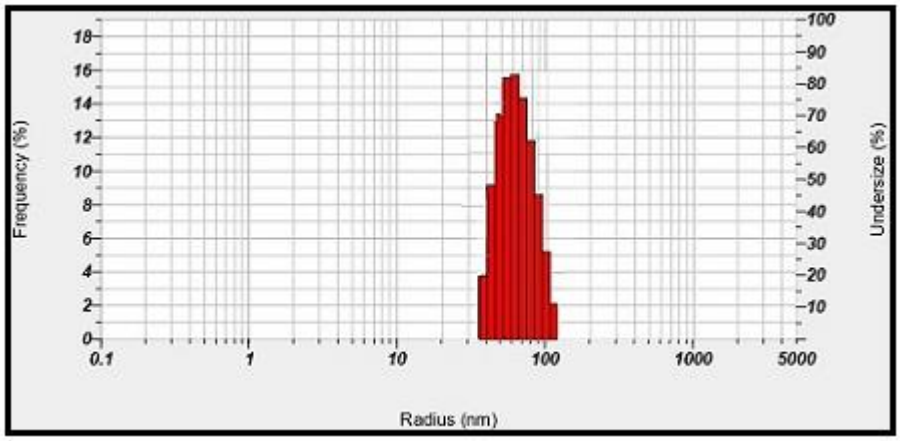


Fig. 5. Particle size image of CuO-NPs

***Anti-microbial activity***

The size and dosage of nanoparticles play a crucial role in determining their antibacterial activity. CuO-NPs exhibit greater activity against Gram-positive bacteria compared to Gram-negative bacteria. As shown in Figure 6, the synthesized CuO-NPs were tested against human bacterial pathogens, including *Klebsiella pneumoniae* (MTCC 109), *Staphylococcus aureus* (MTCC 96), *Pseudomonas aeruginosa* (MTCC 1688), and *Staphylococcus epidermidis* (MTCC 435). According to Table 4, the zone of inhibition for antibacterial activity against Gram-positive bacteria ranged from 9 to 11 mm in diameter. In comparison, the zone for Gram-negative bacteria ranged from 6 to 8 mm. These results indicate that the synthesized CuO nanoparticles are more effective at inhibiting the growth of Gram-positive bacteria than Gram-negative bacteria.

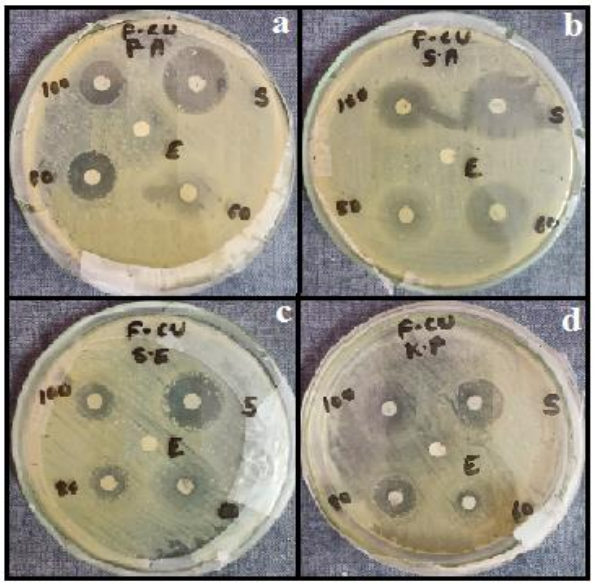


Fig. 6. Antibacterial activity of CuO-NPs against *P.aeruginosa (a), S.aureus (b), S.epidermis(c) and K. pneumonia(d)*

Table 4. *In Vitro* Antibacterial activity of CuO-NPs

| Samples | Conc (µg/ml) | Organisms/Zone of inhibition (mm) | | | |
|---|---|---|---|---|---|
| | | ***P. aeruginosa*** | ***S. aureus*** | ***S. epidermis*** | ***K. pneumonia*** |
| **CuO-NPs** | 60 | 2 | 6 | 3 | 3 |
| | 80 | 7 | 8 | 6 | 5 |
| | 100 | 8 | 11 | 9 | 6 |
| **Std** Amoxicillin | 10 µl/disc | 12 | 14 | 13 | 9 |

Individuals on antifungal medications or those with immune suppression are at higher risk of death due to fungal infections. As shown in Table 5 and Figure 7, the CuO nanoparticles demonstrated a moderate zone of inhibition against *Aspergillus flavus* (5 mm) and *Aspergillus niger* (4 mm), compared to *Candida albicans* (8 mm) and *Candida vulgaris* (7 mm), when treated with conventional amoxicillin.

Table 5. *In Vitro* Antifungal activity of CuO-NPs

| Samples | Concentrations (µg/ml) | Organisms/Zone of inhibition (mm) | | | |
|---|---|---|---|---|---|
| | | ***A. flavus*** | ***C. albicans*** | ***C. vulgaris*** | ***A. niger*** |
| **CuO-NPs** | 60 | 0 | 0 | 2 | 0 |
| | 80 | 2 | 2 | 4 | 1 |
| | 100 | 5 | 8 | 7 | 4 |
| **Standard** Amoxicillin | 10 µl/disc | 7 | 9 | 8 | 6 |

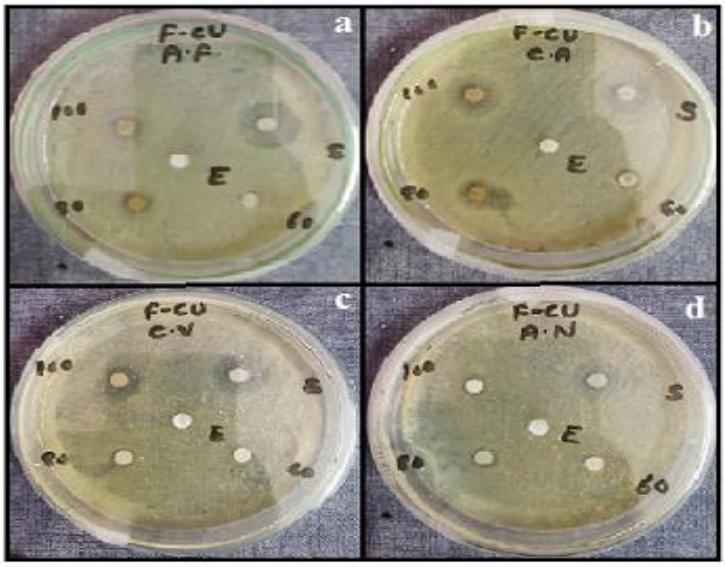


Fig. 7. Antifungal activity of CuO-NPs against *A.flavus(a), C.albicans (b), C.vulgaris(c) and A.niger(d)*

MIC studies are conducted to assess the full dilutions of solutions and determine the lowest concentration of a substance that exhibits antibacterial activity. In this study, the MIC values of synthesized CuO-NPs for *Escherichia coli* and *Streptococcus aureus* were 40 µg/mL and 20 µg/mL, respectively, as shown in Table 6. As indicated in Figures 8 and 9, no discernible growth of the test organisms was observed at the lowest concentrations. These results suggest the potential for in vivo applications.

Table 6. MIC of Fruit extract

| BACTERIA | MIC (µg/ml) |
|---|---|
| *Escherichia coli* | 40 |
| *Streptococcus aureus* | 20 |

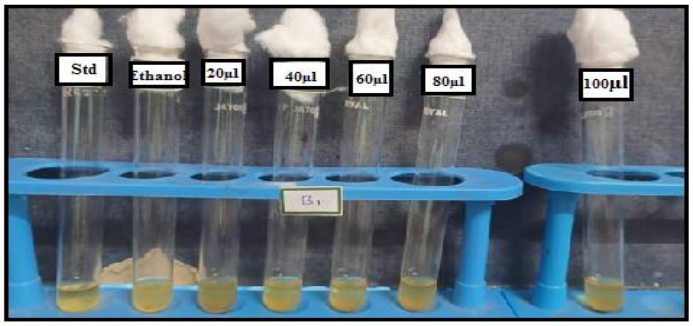


Fig. 8. MIC determination of fruit extracts against *Escherichia coli*

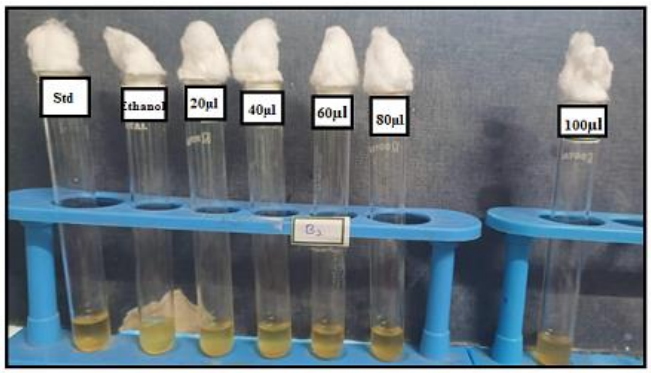


Fig. 9. MIC determination of fruit extracts against *Streptococcus aureus*

***Anti-oxidant analysis***

After testing the produced nanoparticles for antioxidant activity, it was found that CuO-NPs exhibited significant antioxidant properties, as shown in Figures 10 and 11. According to Table 7, the CuO-NPs demonstrated a scavenging activity of 80.39% at 100 µg/mL. As the concentration of CuO-NPs increased, so did the antioxidant activity, with an IC50 value of 49.92%. These results suggest that the synthesized CuO nanoparticles regulate oxidative stress caused by wounds, thereby facilitating the healing process.

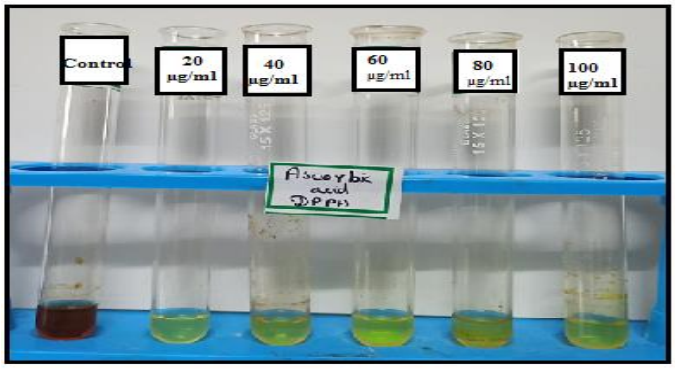


Fig. 10. Antioxidant activity of Ascorbic acid by DPPH assay method

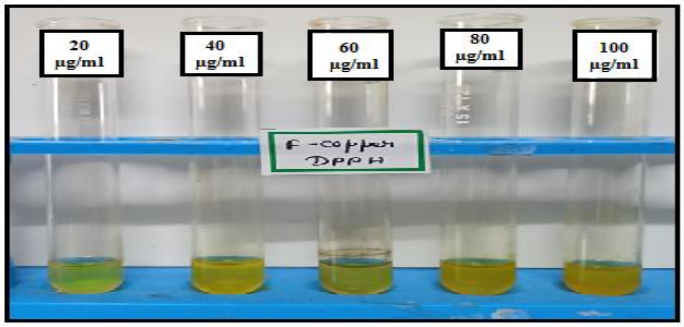


Fig. 11. Antioxidant activity of CuO-NPs by DPPH assay method

Table 7. Percentage of inhibition

| S.No | Concentration (µg/ml) | Antioxidant activity DPPH% | |
|---|---|---|---|
| | | CuO-NPs | Ascorbic acid |
| 1. | 20 µg/ml | 38.23 | 47.05 |
| 2. | 40 µg/ml | 47.05 | 59.80 |
| 3. | 60 µg/ml | 53.92 | 65.68 |
| 4. | 80 µg/ml | 59.80 | 71.56 |
| 5. | 100 µg/ml | 80.39 | 88.23 |
| | **$IC_{50}$ Value** | **49.92** | **22.04** |

***In vivo wound healing activity***

***Body weight***

The body weight of the animals was monitored on days 0, 1, 7, 14, 21, and 28, as shown in Table 8 and Figure 12. No significant changes in body weight were observed throughout the study, with all animals showing a normal increase in weight.

Table 8. Effect of CuO-NPs Ointment on Body weight

| Groups | Body weight (g) | | | | | |
|---|---|---|---|---|---|---|
| | Day 0 | Day 1 | Day 7 | Day 14 | Day 21 | Day 28 |
| Group I-Control | 180.17±4.26 | 180.33±4.18 | 184.17±3.25 | 188.00±3.29 | 191.17±3.06 | 195.67±2.16 |
| Group II- CuO-NPs | 182.83±3.49 | 183.50±3.56 | 186.33±3.43 | 188.67±2.73 | 193.17±1.47 | 198.50±3.39 |

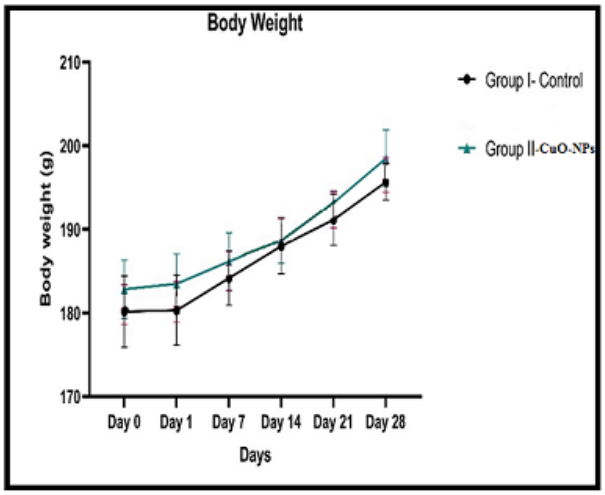


Fig. 12. Effect of CuO-NPs Ointment on body weight

***Assessment of wound healing***

The wound area was measured on days 0, 1, 7, 14, 21, and 28, as shown in Table 9 and Figure 13a. No difference in the wound area was observed on days 0 and 1. However, on days 7, 14, 21, and 28, Group II exhibited a smaller wound area compared to Group I. Group II's wound area showed significant improvements when compared to Group I. Table 10 and Figure 13b illustrate the calculation of the percentage of wound closure on days 0, 1, 7, 14, 21, and 28. Group II demonstrated more significant and prominent wound closure on days 7, 14, 21, and 28 compared to the control group (Group I), as depicted in Figure 14 and 15.

Table 9. Effect of CuO-NPs Ointment on Wound Area ($mm^2$)

| Groups | Wound area ($mm^2$) | | | | | |
|---|---|---|---|---|---|---|
| | Day 0 | Day 1 | Day 7 | Day 14 | Day 21 | Day 28 |
| Group I-Control | 498.33±2.16 | 495.00±2.10 | 408.50±12.47 | 297.50±10.93 | 161.50±13.66 | 52.50±9.05 |
| Group II- CuO-NPs | 498.67±2.66 | 492.50±2.07 | 310.50±5.96* | 106.50±10.63* | 5.67±2.42* | 0.67±0.82* |

Table 10. Effect of CuO-NPs Ointment on Percentage wound closure

| Groups | Percentage wound closure (%) | | | | | |
|---|---|---|---|---|---|---|
| | Day 0 | Day 1 | Day 7 | Day 14 | Day 21 | Day 28 |
| Group I-Control | 0±0 | 0.94±1.03 | 41.04±2.68 | 64.24±1.62 | 85.70±2.33 | 96.07±0.82 |
| Group II- CuO-NPs | 0±0 | 1.08±0.33 | 53.82±1.77* | 82.59±1.02* | 99.50±0.21* | 100.00±0* |

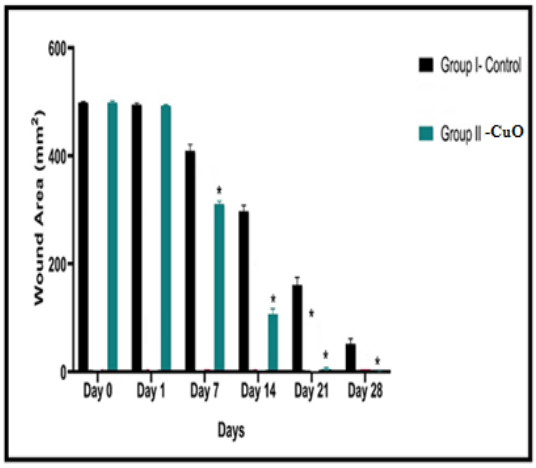


Fig. 13. Effect of CuO-NPs Ointment on Wound area ($mm^2$)

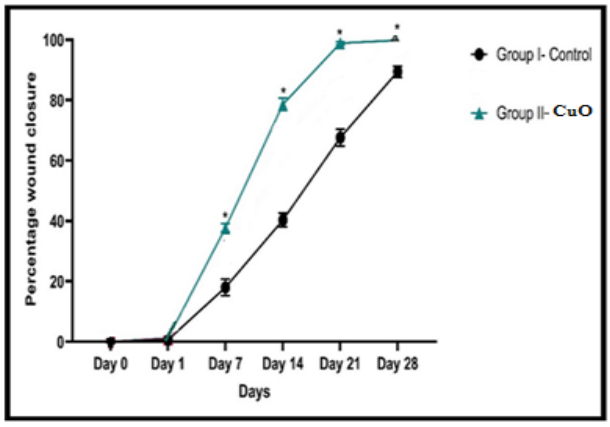


Fig. 14. Effect of CuO-NPs Ointment on Percentage Wound Closure

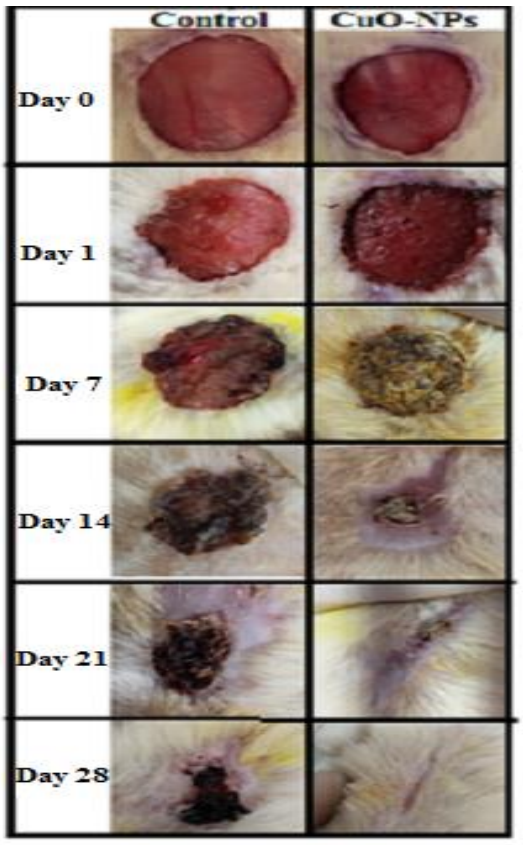


Fig. 15. Effect of CuO-NPs Ointment on wound closure

***Histopathology***

The histological characteristics of the skin tissue from each animal in the group were examined under a Motic microscope (20x). As shown in Figure 16, animals in Group I (control) exhibited prominent scar tissue, along with inflammatory cells, fibroblast cells, decreased collagen fibers, and blood vessels. In contrast, Group II displayed increased blood vessels, collagen fibers, and fibroblast cell renewal in the tissues. Group II demonstrated a greater degree of wound healing compared to Group I (control).

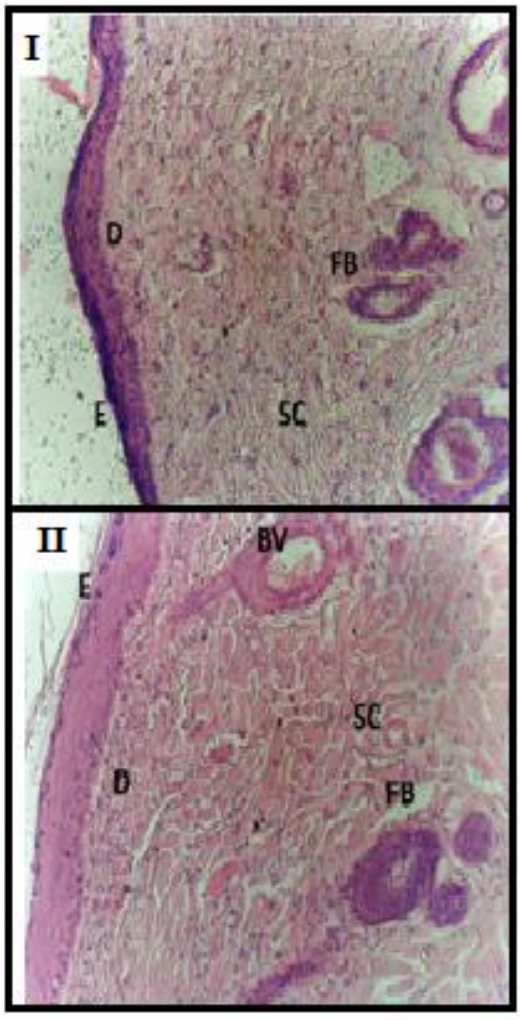


Fig. 16. Histopathological evaluation of skin tissue I) Group I-Control; II) Group II-Cu; **E-**Epidermis, **D**-Dermis, **SC-** Subcutaneous, **BV**-Blood vessels, **FB-** Fibroblast cell

## CONCLUSION

A wound is a serious medical condition that, if left untreated, can lead to infections. CuO nanoparticles synthesized from *D. palmatus* fruit extract show great potential as effective and less harmful therapeutic agents. Characterizing CuO nanoparticles using ultraviolet-visible spectroscopy, FT-IR, XRD, SEM-EDX, and DLS particle size analysis confirms the presence of biomolecules responsible for forming copper oxide nanoparticles. CuO-NPs exhibit greater antibacterial efficacy against Gram-positive bacteria such as *Staphylococcus aureus* and *Staphylococcus epidermidis*, compared to Gram-negative bacteria like *Pseudomonas aeruginosa* and *Klebsiella pneumoniae*. Candida vulgaris and Candida albicans showed a larger inhibition zone than Aspergillus species regarding antifungal activity. The synthesized CuO-NPs demonstrated potent antioxidant activity by effectively scavenging free radicals, which aids in regulating oxidative stress and promotes wound healing. Over 28 days, compared to Group I (control), CuO nanoparticles derived from *D. palmatus* fruit extracts significantly reduced wound area, enhanced wound closure, and exhibited improved histological results. The findings of this study conclude that CuO-NPs synthesized from *D. palmatus* fruit extracts possess robust antibacterial, antioxidant, and wound-healing properties. CuO-NP-based nanoemulsions promote wound healing at various stages of the healing process. These results open new avenues for medical research and suggest that CuO nanoparticles could be used to develop advanced antimicrobial medications and wound-healing ointments.

## ETHICAL APPROVAL

Ethical Committee: Centre of Advanced drug Research and Testing, JSS college of pharmacy, Ooty. CPCSEA - Ministry of Environment and Forest, Government of India, approved. Approval number – JSSCP/OT/IAEC/53/2023-24.

## CONSENT FOR PUBLICATION

Not applicable.

## AVAILABILITY OF DATA AND MATERIALS

All data generated or analyzed during this study are included in this published article.

## CONFLITS OF INTEREST

The authors declare no competing interests.

## AUTHOR CONTRIBUTION

G.T.P. was involved in conceptualization and original draft preparation, P.R. supervised the project, S.K. was engaged in the experimental part, and M.B. and V.V. were involved in microbial testing.

## ACKNOWLEDGEMENT

We thank Dr.Praveen T. Krishnamurthy, Professor and Head, Department of Pharmacology, and JSS College of Pharmacy, Ooty's institutional committee, for providing the animal facility.

## FUNDING

This research received no specific grant from any funding agency in the public, commercial, or not-for-profit sectors.



## REFERENCES

1. Lesong Conteh, Thomas Engels, David H Molyneux. Socioeconomic aspect of neglected tropical diseases. Lancet.2010:375:239-247
2. Ikuta KS, Swetschinski LR, Robles Aguilar G, Sharara F, Mestrovic T, Gray AP, Davis Weaver N, Wool EE, Han C, Gershberg Hayoon A. (GBD 2019 Antimicrobial Resistance Collaborators), Global mortality associated with 33 bacterial pathogens in 2019: a systematic analysis for the Global Burden of Disease Study 2019. Lancet. 2022; 400(10369):2221-22248.
3. R. B. McaFee, Disease-A-Month journal, Elsevier.2013; 59:426
4. Cossart YE. The rise and fall of infectious diseases: Australian perspectives, 1914-2014. Med J Aust. 2014; 201(S1):S11-S14
5. Murray CJ, Richards MA, Newton JN, Fenton KA, Anderson HR, Atkinson C, Bennett D, Bernabé E, Blencowe H, Bourne R, Braithwaite T. UK health performance: findings of the Global Burden of Disease Study 2010. Lancet.2013; 381:997-1020
6. Kirsner RS. The Wound Healing Society chronic wound ulcer healing guidelines update of the 2006 guidelines--blending old with new. Wound Repair Regen. 2016; 24(1): 110.
7. Moghadamtousi SZ, Rouhollahi E, Hajrezaie M, Karimian H, Abdulla MA, Kadir HA. Annona muricata leaves accelerate wound healing in rats via involvement of Hsp70 and antioxidant defence. Int J Surg. 2015; 18:110-117
8. Sumitha S, Vidhya R, Lakshmi MS, Prasad KS. Leaf extract mediated green synthesis of copper oxide nanoparticles using Ocimum tenuiflorum and its characterization. Int J Chem Sci. 2016; 14(1):435-440.
9. Mohan S, Singh Y, Verma DK, Hasan SH. Synthesis of CuO nanoparticles through green route using Citrus limon juice and its application as nanosorbent for Cr (VI) remediation: Process optimization with RSM and

ANN-GA based model. Process Saf Environ Prot. 2015; 96: 156-166.
10. Kavitha K, Baker S, Rakshith D, Kavitha H, Yashwantha Rao H, Harini B, Satish S. Plants as green source towards synthesis of nanoparticles. Int Res J Biol Sci. 2013, 2, 66–76.
11. Yuvakkumar R, Hong S. Green Synthesis of Spinel Magnetite Iron Oxide Nanoparticles. Adv Mater Res. 2014, 1051, 39–42.
12. Kalashnikova I, Das S, Seal S. Nanomaterials for wound healing: scope and advancement. Nanomed. 2015; 10(16):2593–2612.
13. Barroso A, Mestre H, Ascenso A, and Simões S, Reis C. Nanomaterials in wound healing: From material sciences to wound healing applications. Nano Select. 2020; 1:443-460.
14. Wang X, Chang J, Wu C. Bioactive inorganic/organic nanocomposite for wound healing. Appl Mater Today. 2018; 11:308–319.
15. Nasrollahzadeh M, Sajadi S.M. Green synthesis of copper nanoparticles using Ginkgo biloba L. leaf extract and their catalytic activity for the Huisgen (3 + 2) cycloaddition of azides and alkynes at room temperature. J Colloid Interface Sci. 2015; 457: 141–147.
16. Badriyah Alotaibi et al. Green synthesized Cu-Oxide nanoparticles: Properties and applications for enhancing healing of wounds infected with Staphylococcus aureus. Int J Pharm.2023; 645:123451
17. Germplasm Resources Information Network. Diplocyclos palmatus (L.) C. Jeffrey. Published-Kew Bull. 15:352.1962
18. Michel H. Sorting Diplocyclos Names. Multilingual Multiscript Plant Name Database –A Work in Progress. School of griculture and Food Systems. The University of Melbourne; 2010.
19. Attar UA, Ghane SG. Phytochemicals, antioxidant activity and phenolic profiling of Diplocyclos palmatus (L.) C. Jeffery. Int J Pharm Pharm Sci.2017; 9:101-106
20. Agrawal SS, Paridhavi M. Herbal Drug Technology. 2nd ed. Mumbai: Dattani Book Agency; 2014.
21. Renuka K, Devi VR, Subramanian SP. Phytochemical screening and evaluation of in vitro antioxidant potential of immature palmyra palm (Borassus flabellifer Linn) fruits. Int J Pharm Pharm Sci. 2018; 10:77-83.
22. Tambekatr D.H. and M.A. Kharate. Studies on antimicrobial properties of leaves extract of some edible plants. Asian J Mol Biol Environ Sci. 2005; 7(4): 867-872.
23. RajeshKumar S, Rinitha G. Nanostructural characterization of antimicrobial and antioxidant copper nanoparticles synthesized using novel Persea americana seeds. Open Nano. 2018;3: 18-27.
24. Raka SC, Rahman A, Kaium MK. Evaluation of antioxidant and antimicrobial activity of methanolic extract of Ficus fistulosa leaves: an unexplored phytomedicine. PharmacologyOnline. 2019;1:354-360.
25. Acharya, K., Samui, K, Rai, M. Antioxidant and nitric oxide synthetase activation properties of Auricularia auricular. Indian J Exp Biol. 2004; 42, 538-540.
26. Stefanovits-Bányai É. Antioxidant effect of various rosemary (Rosmarinus officinalis L.) clones. Acta Biologica Szegediensis. 2003;47(1-4):111-3.
27. Pawar RS, Chaurasiya PK, Rajak H, Singour PK, Toppo FA, Jain A. Wound healing activity of Sida cordifolia Linn in rats. Indian J Pharmacol. 2013; 45(5):474-478.
28. Lakshmi Prabha K, Jayashree M, Shakila Banu K, Gino A Kurian. Green and chemically synthesized copper oxide nanoparticles-A preliminary research towards its toxic behavior. Int J Pharm Pharm Sci. 2015; 7(1), 156-160.
29. Alminderej FM. Study of new cellulosic dressing with enhanced antibacterial performance grafted with a biopolymer of chitosan and myrrh polysaccharide extract. Arab J Chem. 2020; 13: 3672–3681.
30. Xu D, Zhu C, Meng X, Chen Z, Li Y, Zhang D, Zhu S. Design and fabrication of Ag-CuO nanoparticles on reduced graphene oxide for nonenzymatic detection of glucose. Sensors and Actuators B: Chemical. 2018; 265:435-442.
31. Ssekatawa K, Byarugaba DK, Angwe MK, Wampande EM, Ejobi F, Nxumalo E, Maaza M, Sackey J, Kirabira JB. Phyto-mediated copper oxide nanoparticles for antibacterial, antioxidant and photocatalytic performances. Front Bioeng Biotechnol. 2022;10:820218.